UCRL-JC-151573

LAWRENCE
LIVERMORE
NATIONAL
LABORATORY

Self Thomson Scattering in Laser Produced Plasmas

C. Niemann, S.H. Glenzer, R.L. Kauffman, N.B. Meezan, K. Oades, G. Slark, M. Stevenson, and L.J. Suter

August 22, 2003

3rd International Conference on Inertial Fusion Sciences and Applications, Monterey, California, September 7-12, 2003

Self Thomson scattering in laser produced plasmas

C. Niemann*, S.H. Glenzer*, R.L. Kauffman*, N.B. Meezan*, K. Oades†, G. Slark†, M. Stevenson† and L.J. Suter*

*Lawrence Livermore National Laboratory, 7000 East Avenue, Livermore, CA 94550
†Atomic Weapon Establishment, Aldermaston, Reading, RG74PR, UK

Abstract. An imaging Thomson-scattering diagnostics has recently been implemented at the *Helen* laser facility of the *Atomic Weapon Establishment (AWE)*. Laser produced plasmas are simultaneously created, heated and diganosed with a single 400 J / 1 ns heater beam at 2ω (526.6 nm). Self scattered light from the heater beam was collected at a scattering angle of 90^o and imaged onto the entrance slit of an imaging spectrometer to obtain spatially and temporally resolved Thomson scattering spectra. We present measurements of electron temperature and temperature gradients in the blow-off plasma of Au-hohlraum targets as well as gas-filled micro-balloons (gasbags) filled with C_5H_{12}, Ne and N_2.

Self-Thomson scattering in laser produced plasmas may be developed into a powerfull technique to measure the electron temperature, temperature gradients as well as the laser-beam propagation through an underdense plasma [1, 2, 3]. Indirect drive inertial confinement fusion depends on efficient propagation of high intensity laser beams through gas-filled closed-geometry hohlraums. As part of collaborative experiments at the Helen laser facility to explore the utility of 2ω laser light for the National Ignition Facility (NIF) we implemented an imaging self-Thomson scattering diagnostics to assess the applicability of self-Thomson scattering on early experiments on NIF.

In these experiments, we apply a single 400 J laser beam at 2ω (526.6 nm frequency doubled from 1054 nm) in a 1 ns square pulse and focus the beam with an f/3.2 lens and a phase plate (PZP) onto a gasbag [4] or a Au-hohlraum target. Using different PZPs the beam diameter at focus can be adjusted between 40 μm and 500 μm, with maximum laser intensities of 10^{15} W/cm^2. Light from the heater beam which is self-scattered in the plasma is collected and collimated by an achromatic f/3 collection lens (f=120 mm, D=30 mm) mounted at an angle of 90^o relativ to the laser beam (Fig. 1 **a**). A second lens (f=500 mm, D=60 mm) images the plasma onto the slit of a half-meter imaging spectrometer with a magnification of 1:4. Using a periscope, the laser-beam propagation direction is projected along the hight of the spectrometer slit in order to allow space resolved Thomson scattering measurements with a spatial resolution of 50 μm. A 1200 grooves/mm grating operated in the second order in combination with a 100 μm spectrometer slit gave a spectral resolution of 0.05 nm. The spectrometer exit plane was imaged onto an S20 image intensified gated optical imager (GOI) with a gate width of 125 ps. The spectra were recorded on photographic film (TMAX, 3200 ASA) and digitized for further analysis. The scattering volume is defined by the total magnification of the optical system, the spectrometer slit width and the heater beam diameter inside the target (defined by the PZP and the plasma induced beam-spread). The 1 mm long field of view was located in that half of the 2.2 mm wide gasbag, where the laser beam enters (Fig. 1 **b**). We directly measure the electron temperature and longitudinal temperature gradients along the laser beam (z-axis) within the field of view. The integration of the scattered light intensity across the heater beam diameter (y-axis) and thus the transverse temperature gradients $\partial T/\partial y$ leads to a broadening of the Thomson-scattering spectrum and to a dependence of the spectra on possible beam filamentation (see below).

For our plasma parameters, the scattering parameter is $\alpha = 1/(k\lambda_D) > 2$ and the scattering is collective ($k = 4\pi/\lambda_0 \cdot sin(\Theta/2)$, $\Theta = 90^o$ is the scattering angle and λ_D is the Debye length). For these conditions the calculated scattering spectrum shows two ion acoustic peaks, symmetrically arranged around the wavelength of the laser beam ($\lambda_0 = 526.6$ nm), where the wavelength separation $\Delta\lambda$ of the two peaks increases with the electron temperature ($\Delta\lambda \sim \sqrt{Z \cdot T_e}$, Z is the charge state). However, the measurements in the blow-off plasma of Au-hohlraum targets show multiple ion acoustic peaks (Fig. 2, # 1 to 4) corresponding to different temperatures. At $z = 0.38$ mm we observe temperatures between 140 eV (#1) and 1.3 keV (#4). The maximum temperature increases from only a few tens of eV at z=0 to more than 1

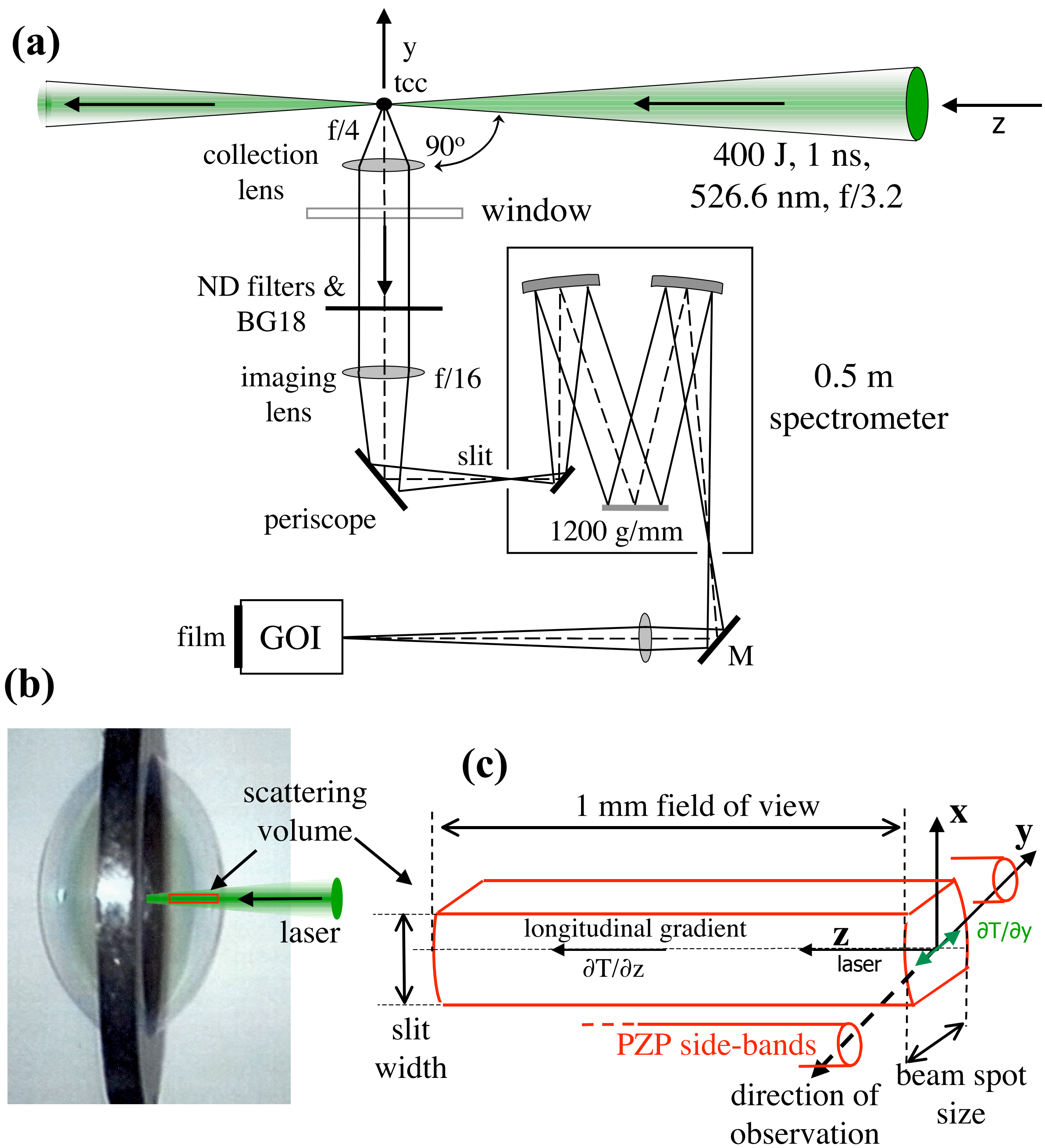

FIGURE 1. Setup of the imaging self-Thomson scattering diagnostics at Helen **(a)** , location of the scattering volume inside the gasbag target **(b)** and the scattering geometry **(c)**.

keV near the laser entrance hole of the hohlraum ($z > 0.6$ mm), with a temperature gradient of up to 2.5 keV/mm. In addition, we interpret the existance of multiple peaks as signature of beam filamentation and the contribution of the PZP side-bands. The plasma induces a break-up of the beam into several intense filaments that create and thus probe distinct cells in the plasma with different temperature. In particular the PZP side-bands probe the colder outer regions of the plasma (Fig. 1 **c**) and contribute to the low temperature ion-acoustic peaks in the scattering spectrum. Due to the transmission of the spectrometer-GOI system, the blue half of the spectrum is cut below 526.5 nm. The synthetic spectrum, which is compared to the measurement in Fig. 2 was calculated

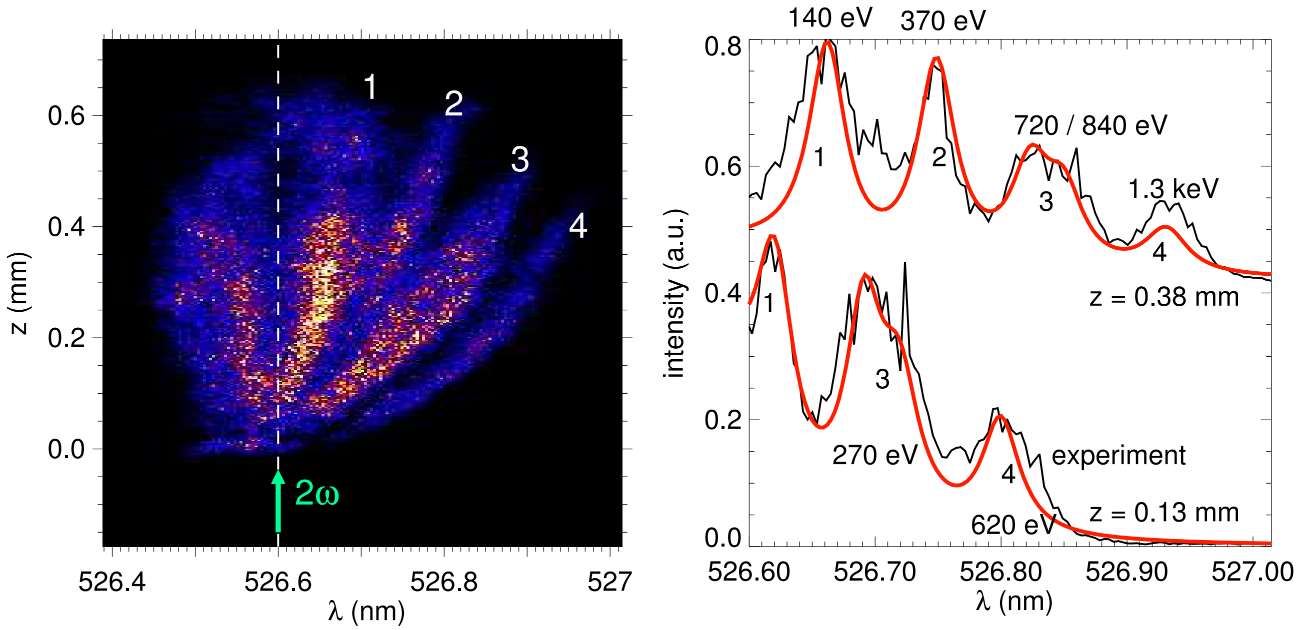

FIGURE 2. Spatially resolved self-Thomson scattering spectrum of the blow-off plasma from a Au-Hohlraum and the lineouts for $z = 0.13$ *mm* and 0.38 *mm* (only the redshifted spectrum). The beam enters from the bottom (negative z). The laser entrance hole is located outside the field of view (z>0.6 mm). The red solid line in the right graph shows the theoretical spectrum, calculated from a superposition of four different spectra with different temperature and scattering intensity.

from the standard theoretical form factor [5], superimposing several different Thomson scattering spectra with different temperatures and scattering intensity.

In low density (n_e/n_c =5%, where $n_c = 4 \cdot 10^{21}$ cm^{-3} is the cut-off density for 2ω laser light) neon-gasbags, we observe a very simmilar behaviour. Multiple peaks, corresponding to a multitude of ion-acoustic features originating from light scattered from plasma regions with different temperature form a broad spectrum with a maximum observable temperature of 1.1 keV and a longitudinal temperature gradient above 2 keV/mm (Fig. 3). Low density nitrogen-gasbags (n_e/n_c =4%) show maximum observable electron temperatures of 530 eV and temperature gradients up to 1.3 keV/mm.

In low density pentane-gasbags (C_5H_{12}) we observe a maximum temperature of 440 eV. This value is low compared to hydrodynamic simulations [6]. At higher densities between 10% and 25% n_c, the measurable temperatures drop even further. At the highest investigated density of 1/4 n_c the maximum observable temperature is only a few tens of eV. According to hydrodynamic simulations, the temperature in the center of the plasma increases slightly with the density [6]. Light scattered from the hot central region of the plasma is absorbed in the high density plasma that is created around the heater beam due to hydrodynamic expansion [6] and does thus not contribute to the Thomson scattering spectra significantly.

Improvements of these measurements, such as a larger field of view, a higher dynamic range, or shorter probe-laser wavelength will be advantageous to use this technique on NIF for the study of electron temperatures and laser beam propagation.

This work was performed under the auspices of the U.S. Department of Energy by the University of California Lawrence Livermore National Laboratory under Contract No. W-7405-ENG-48.

REFERENCES

1. H.J. Kunze, in *Plasma Diagnostics*, edited by W. Lochte-Holtgreven (North-Holland, Amsterdam, 1968), p. 550
2. S.H. Glenzer et al., Phys. Plasmas, **6** (5), 2117 (1999)
3. A.W. DeSilva and G.C. Goldenbaum, in *Methods of Experimental Physics*, edited by H.R. Griem and R. Lovberg (Academic, New York, 1967), Sec. V9A
4. B.J. MacGowan et al., Phys. Plasmas **3**, 2029 (1996)
5. D.E. Evans and J. Katzenstein, Rep. Prog. Phys. **32**, 207 (1969)
6. N.B. Meezan et al., this proceedings

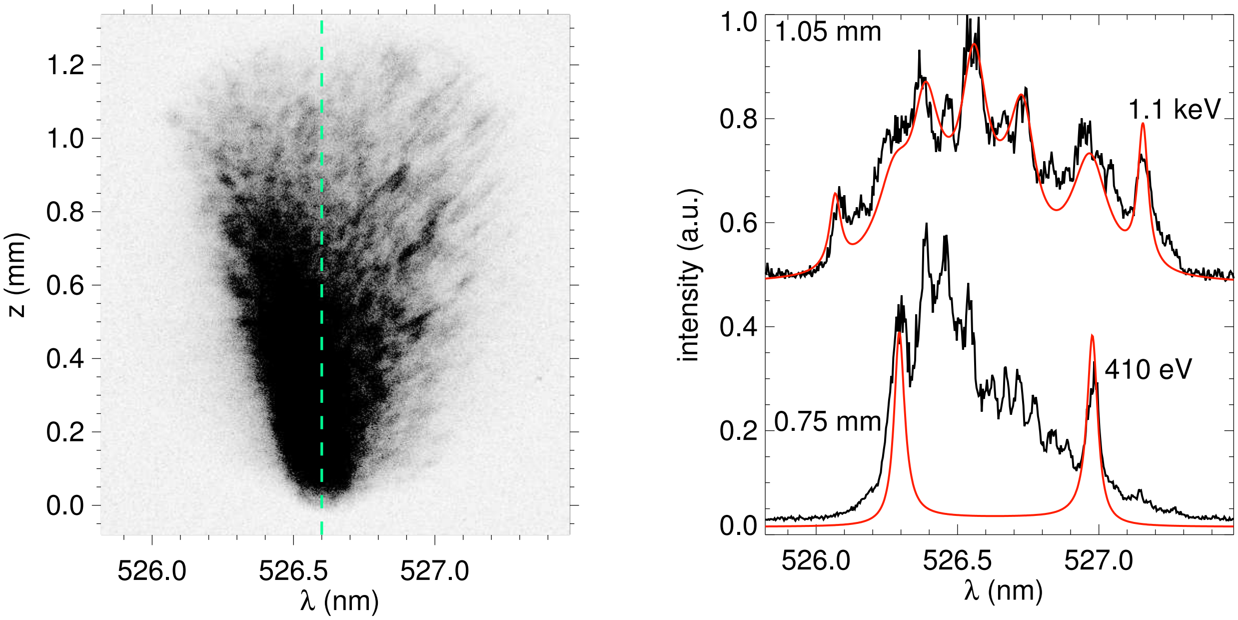

FIGURE 3. Thomson scattering spectrum of a ne gasbag at $n_e/n_c = 5\%$ and the lineout for two different positions. The theoretical line is a superposition of Thomson scattering spectra with different temperature, scattering intensity and particle ditribution function. For the z=0.75 mm case, the synthetic spectrum includes only the maximum temperature (410 eV). The low temperature contributions between the two peaks was neglected.

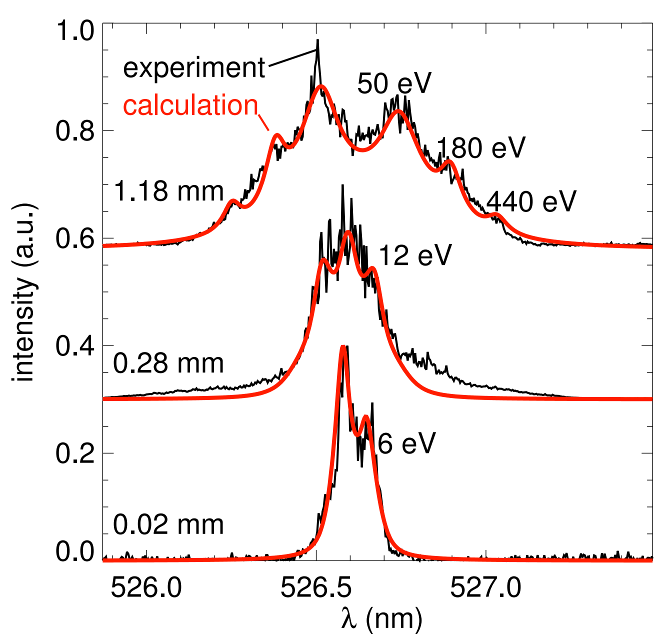

FIGURE 4. Thomson scattering spectra of a C_5H_{12} gasbag at $n_e/n_c = 4\%$ at three different positions along the heater beam.